Body Measurement System using White Light Projected Patterns for Made-to-Measure Apparel

Jeffery D. Hurley[a], Michelle H. Demers[a], Richard C. Wulpern[a], John R. Grindon[b]

[a]Textile/Clothing Technology Corporation, Cary, North Carolina
[b]John R. Grindon & Assoc., Hazelwood, Missouri

ABSTRACT

A non-contact body measurement system (BMS) is under development for use in making made-to-measure apparel, and for other applications related to body measurement. The BMS design is discussed which consists of six stationary structured-light projectors and six CCD cameras utilizing a phase-shifting technique. The solution for calculating three-dimensional surface points of a human body from the camera images is described. A statistical error analysis is summarized for the phase measurement error due to image noise. The phase errors due to image and pattern quantizations are analyzed. The effect of phase measurement error upon the three-dimensional point solution is shown in terms of the system parameter values. An operating development implementation of the BMS is described and pictured. Contour plots of test subjects taken with this system, showing digitized three-dimensional surface segments, are presented and discussed.

Keywords: 3D image capture, 3D surface digitization, phase measurement profilometry, custom clothing, anthropometry

1. INTRODUCTION

In order to be more competitive in the world market, the US apparel industry, is considering a move toward mass customization. This move requires a method for accurately obtaining human body measurements and extracting the appropriate critical measurements so that patterns can be altered for the customer. Tailors have traditionally taken these measurements themselves for their own pattern altering methods, but these measurements are notoriously inconsistent when compared with other tailors' measurements. For mass customization to succeed, accurate and consistent measurements of the customer's body is needed. Some of the technologies that have been used for body measurement include 2D video silhouette images, laser based scanning, and white light phase measurement. The white light phase measurement approach was chosen in this research effort to get a full three-dimensional representation of the body without the use and cost of lasers. The structured light and phase measurement profilometry (PMP) application is well suited for body measurement because of the short acquisition time, accuracy, and relatively low cost. PMP using structured white light was first introduced in 1986 by M. Halioua in Ref. 1, and it required prior knowledge of the image field and continuity of the surface. This paper presents an application of the PMP method with additional algorithms developed that resolve the ambiguous surface discontinuities.

2. OVERVIEW OF BMS

2.1 BMS Design

The design of the BMS is driven by the unique coverage requirements imposed by the shape of the human body. For instance, in order to scan a majority of the population, the scanning volume was designed to be 1.1 m wide by 1.0 m thick by 2.0 m in height. Also more detail and coverage is required on the front surface of the body than on the back surface. For this reason, the BMS was designed with three towers; each tower consisting of a lower and upper sensor. The two front towers with a 60 degree included separation angle and a straight on back tower are shown in Figure 2.1. With this separation angle,

SPIE Vol. 3131 • 0277-786X/97/$10.00

there is overlap between the viewing areas of the towers where detail is needed in high slope regions and minimal overlap on outer edge regions where surfaces are smoother.

The six sensors that view the body are stationary which is different from some laser systems that use moving sensors. This method is used because of the need for a relatively short acquisition time, and moving sensors around a body or moving a body in front of a sensor in a few seconds presents dynamic issues. Since the sensors are stationary, each captures an area segment of the surface, instead of a single contour on the surface. The area segments from each of the sensors are combined to form an integrated surface model which covers at least those critical areas of the body that are needed for extracting measurements used in making apparel.

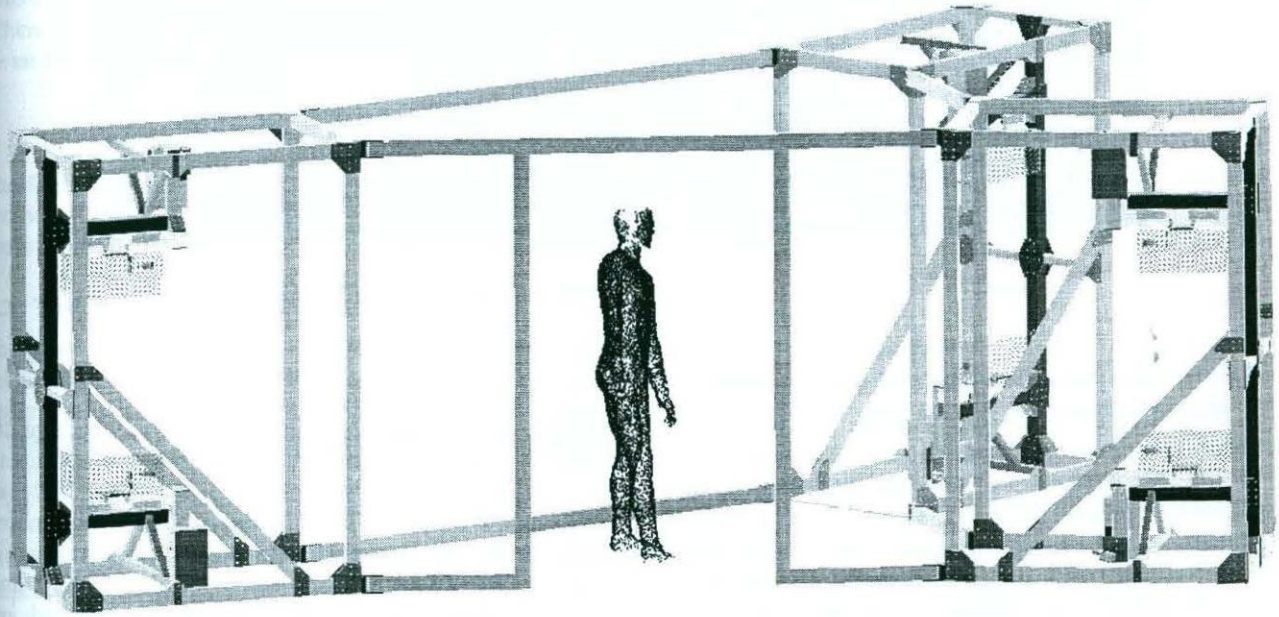

Figure 2.1 Overview of Body Measurement System for made-to-measure apparel.

2.2 BMS Sensor Head Design

The PMP approach is well suited to the needs of the area segment design of the body measurement system. In this approach, a sensor head, which consists of a structured light projector and an area sensing CCD camera, form a vertical triangulation with the object or body. The camera and projector are positioned to achieve the desired total sensing area necessary for mapping points onto the surface of the body. The projector contains a two-dimensional patterned grating which is projected onto the body using a white light source. The pattern varies in intensity sinusoidally in the vertical direction, and is invariant horizontally. Two different sinusoidal grating patterns are used. A coarse grating pattern is used to acquire a rough map of the body. A fine grating pattern, in combination with the coarse pattern results, yields the final surface data of the body. Both projected patterns are imaged using an area array charge-coupled device (CCD) camera, as shown in Figure 2.2.

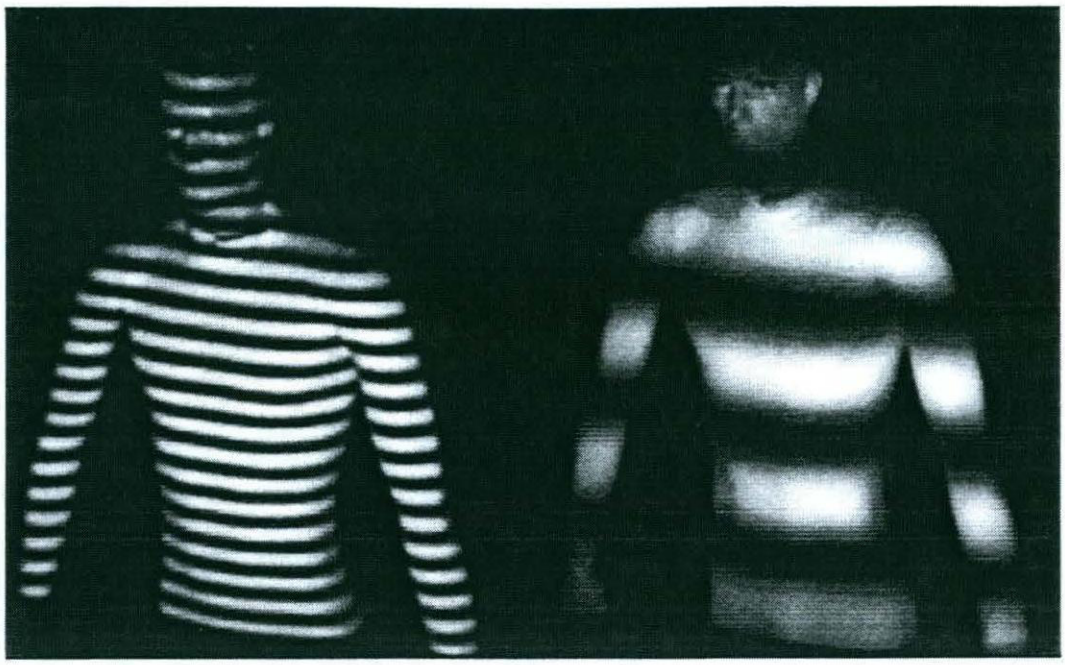

Figure 2.2 Projected sinusoidal patterns from fine and coarse grating.

2.3 BMS System Hardware and Software Design

The BMS structure is designed with an "erector set" approach to enable later adaptability to the changing needs of the system. The structure is built with a black anodized aluminum extrusion and is covered with non-reflective black theater cloth for light tightness and to reduce spurious reflection inside the system. The three viewing angles of the body are achieved by arranging the three towers as shown in Figure 2.1. Each tower contains two of the sensor heads described above to capture the full height of the body. Each sensor head consists of a black anodized aluminum extrusion structure which rigidly holds a custom designed projector, a commercial CCD camera, and the necessary controls for both. The whole system is controlled by a Pentium 133 personal computer. The computer contains 128 MB RAM, a motion control card, and two frame grabber boards. Additional electronics hardware and wiring necessary to interface the computer to the six sensor heads is contained in an enclosure attached to the sensor head.

Four images per sensor head per grating are acquired. Since there are six sensor heads in the BMS, a total of 48 images are captured. In order to minimize the capture time, the computer acquires the images using a round robin acquisition scheme. In this manner, all of the images of the first grating position are captured in succession. After each sensor's image is acquired, the computer starts shifting the respective grating. When all six sensor images are acquired, the sequence is restarted for the next grating position. This process continues until all 24 images have been acquired for the 1mm grating. The gratings are then moved to project the 5 mm grating. The round robin sequence is repeated to acquire 24 images for the 5mm grating. In this manner the critical portion of the scan, which occurs during the 1mm grating acquisition, is captured within 2 seconds.

The software program was developed using Microsoft Visual C++ under the Windows NT platform. The three dimensional graphic display tools were created using the OpenGL graphics library. The software performs the following functions: graphical user interface, controlling the acquisition sequence, acquiring and storing image buffers, processing acquired images and calculating resulting data points, and displaying graphical output.

3. BMS THEORY OF OPERATION

3.1 Phase Shifting

The PMP method involves shifting the grating preset distances in the direction of the varying phase and capturing images at each position. A total of four images is taken for each grating, with the same amount of phase shift, $\pi/2$ radians, of the projected sinusoidal pattern for each image. The phase at each pixel can be determined using the four images of the body. The basic PMP concept is described in Ref. 1. One of the advantages of the PMP method is that the phase value is independent of the ambient light level and the projector's light output. From Ref. 1, the general form of the intensity of the projected pattern is

$$I(x,y) = R(x,y)[A(x,y) + B(x,y)\cos(p(x,y))]$$

where R(x,y) is the object reflectivity, A(x,y) represents the background intensity and B(x,y)/A(x,y) the fringe contrast. When four equal phase shifts of 90 degrees are acquired, the resultant phase as a function of the intensities in the ideal case is given by

$$p = \arctan[(I_4 - I_2)/(I_1 - I_3)]$$

The BMS uses two sinusoidal gratings in each sensor head, "fine" and "coarse". The fine grating has a 1 mm period and provides the required accuracy and depth resolution of the data points. The coarse grating has a 5 mm period and provides gross depth information to resolve any ambiguous phase data from the 1mm grating.

3.2 Three-Dimensional Point Solution

The phase information computed from the four images is used in the calculation of the three-dimensional data points. The calculated phase imaged by each pixel in the CCD array is used to define a specific line of constant phase on the grating pattern. A schematic of the sensor head showing the projected plane from the grating and camera ray from the pixel is shown in Figure 4.1. The phase, p, is related to its spatial location, x_p, on the grating by

$$(p + 2\pi \cdot m) = p_o + 2\pi \cdot r_g \cdot x_p$$

where p_o is the phase at x = 0 on the grating, r_g is the spatial frequency of the sinusoidal pattern, and m is the 2π order with respect to x = 0. The line of constant phase, at location x_p, when projected through the nodal point of the projector lens, $q_{lp} = (x_{lp}, y_{lp}, z_{lp})$, defines a unique plane in space. The equation of this projected plane is given by

$$\begin{bmatrix} z_{lp} & 0 & (x_p - x_{lp}) & -x_p z_{lp} \end{bmatrix} \begin{bmatrix} x \\ y \\ z \\ 1 \end{bmatrix} = 0$$

A pixel location on the CCD array, q_{cc}, combined with the nodal point of the camera lens, q_{lc}, defines a unique ray in space and is given by

$$\begin{bmatrix} x \\ y \\ z \\ 1 \end{bmatrix} = q_{cc} + k(q_{lc} - q_{cc})$$

The parameter k traces points q_s along the ray.

$$q_s = q_{cc} + k\left(q_{lc} - q_{cc}\right)$$

The intersection of the projected plane from the projector and the ray from the CCD pixel defines the parameter k. Substituting k back into the equation for q_c above yields the (x,y,z) location of the imaged surface, which is defined by

$$k = -\frac{\left(z_{lp}x_{cc} + \left(x_p - x_{lp}\right)z_{cc} - x_p z_{lp}\right)}{\left(z_{lp}(x_{lc} - x_{cc}) + (x_p - x_{lp})(z_{lc} - z_{cc})\right)}$$

Now all of the variables are known except the order m of the calculated phase. The order is determined using the coarse 5 mm grating and the predefined location of the scanning area. The 5 mm grating is long enough so that one cycle (0 to 2π) when projected would completely span the depth of the scanning area. For each ray from a pixel in the CCD camera all the possible phases that would fall in the scanning area can be determined. The calculated phase from the four images can then be mapped onto the ray from the camera and its order is thereby determined. Once the order for the imaged phase on the coarse grating is determined, its x_p location is calculated on the grating. This x_p location is then used to resolve the corresponding order of the phase for the fine 1 mm grating. The x_p location on the grating that was determined from the coarse grating should be very close to the x_p location for the fine grating. The fine order is determined from the coarse x_p and the fine phase can be correctly mapped into this order assuming that the difference between the coarse scan and the fine scan is no greater than $\pm\pi$.

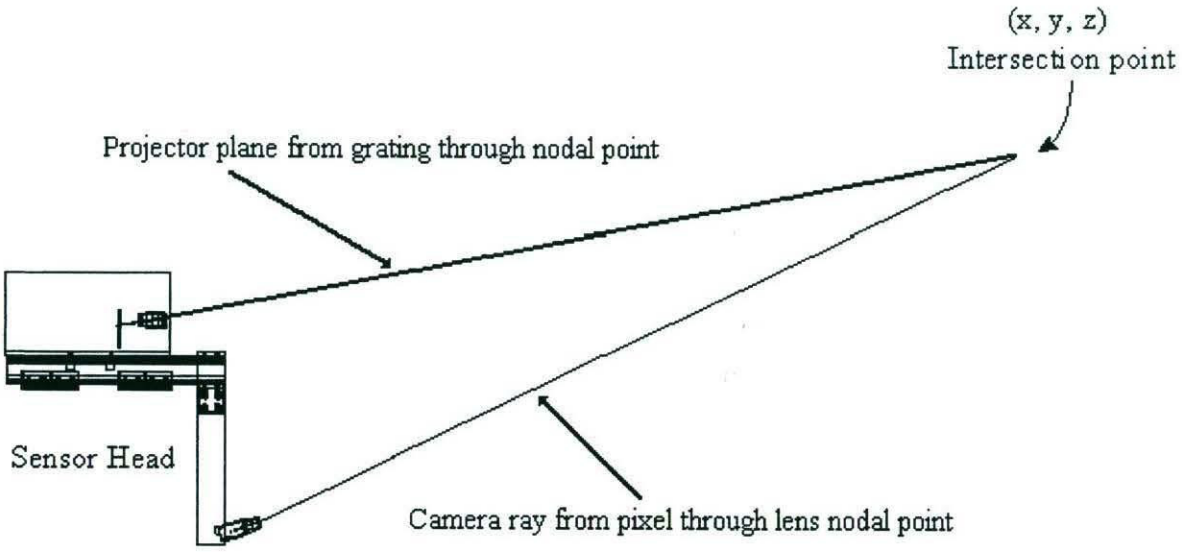

Figure 3.1 Schematic of sensor head with the projected plane and camera ray.

4. ERROR ANALYSIS OF PHASE MEASUREMENT AND DEPTH SOLUTION

For a given sensor, one image is acquired for each of the four projected phase patterns. The intensity values of these four images are processed at each pixel location to produce a phase value at the corresponding imaged point on the subject. In contrast with edge-based pattern methods, such as that described in Ref. 2, the PMP method employs continuously varying amplitude patterns. The amplitude values convey the pattern information. A phase measurement error produces a corresponding error in the depth solution, shown in Section 4.1.

In Ref. 3, the standard deviation of the phase measurement error, std(p), due to an image signal to noise ratio, SNR, was shown for large SNR values to be

$$std(p) = 1 / \left(2 \cdot \sqrt{SNR}\right)$$

The SNR is defined as, $SNR = b^2/(2var(n_o))$, where b is the peak amplitude of the imaged sinusoid and $var(n_o)$ is the image noise variance.

Additional sources of phase error are image amplitude quantization and sinusoidal pattern quantization, both analyzed in Section 4.2.

4.1 Depth Solution Error due to Phase Measurement Error

An error in the phase measurement produces an error in the location the target point position, or depth, along the ray defined by the camera lens nodal point and the position of the pixel in 3D space. Figure 4.1, shows the relevant geometry of the system projected onto an x-y plane. The coordinates of the system are defined as follows: the origin of the xyz coordinate system is defined at the projector lens nodal point, the x axis is defined to pass through the camera lens nodal point at x_c, and the xy plane is defined to pass through the target point at (x_t, y_t). The projector's sinusoidal grating is at an inclination angle of A with respect to the x axis, positioned at a perpendicular distance (focal length, f), from the lens nodal point. The grating is constructed to be invariant along one axis, and oriented so that the invariant axis is nominally parallel to the z axis as the coordinates are defined here. Thus in Figure 4.1, the invariant axis of the grating is perpendicular to the paper. The grating pattern varies sinusoidally along its length in the plane of the paper. The distance, s, on the grating is defined by the phase measurement. If the pitch of the sinusoidal grating is r_g periods per millimeter, and the measured phase is p radians, then the distance s, in millimeters, $s = p / (2\pi r_g)$. The ray passing through the projector lens at the origin from the point at distance s along the grating defines a line at an angle P with respect to the x axis.

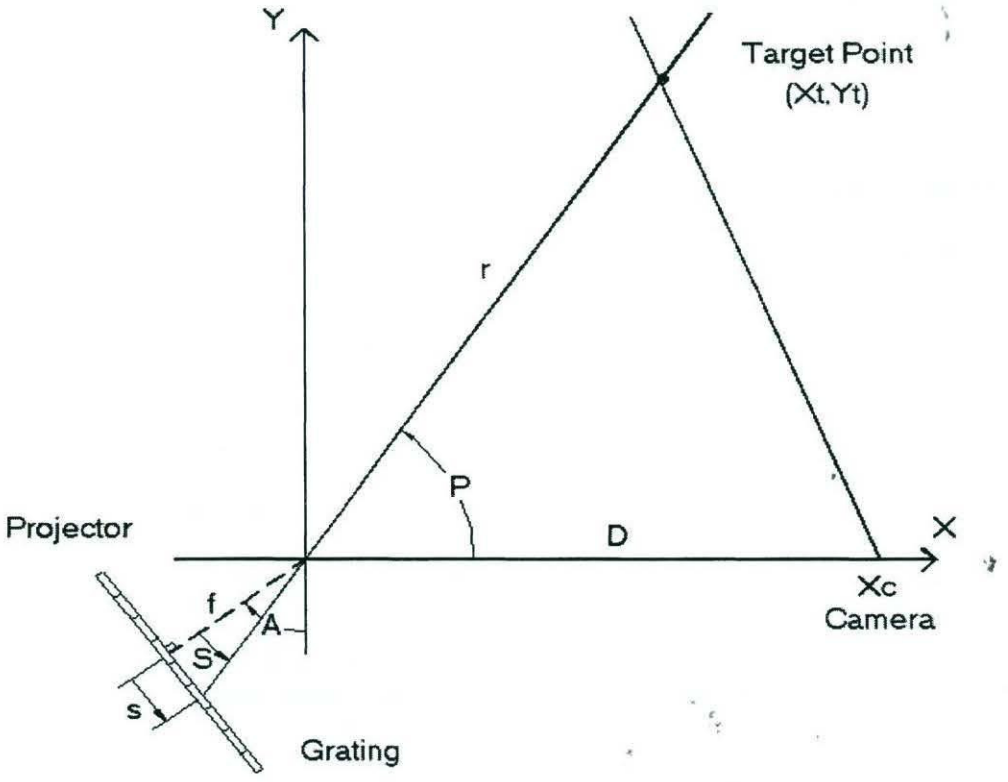

Figure 4.1 Depth Solution Geometry

An angle S = arctan(s / f) is formed by this geometry, as illustrated in Figure 4.1. The angle P is related to angles A and S by $P = S + A + \pi / 2$. The effect of a phase measurement error, dp, is to produce an error dP in the solution for the angle P. First, define the projector constant $c = 2\pi f r_g$. Combining the equations we have S = arctan(p/c). This constant, S, has units of radians, and is a measure of the fineness of the projected pattern. The error in angle P caused by a phase measurement error dp is then, for small errors, found by taking the partial derivative of the angle P with respect to the phase p as follows

$$dP = (c / (c^2 + p^2)) dp$$

where the phase, p, can be expressed in terms of the angle P as $p = c \cot(A - P)$. The standard deviation of the angle P is

$$std(P) = (c / (c^2 + p^2)) std(p)$$

We now have the error in angle P that is caused by a phase error dp. This is expressed in terms of the angle P, the grating inclination A, the projector lens focal length f, and the grating pitch in periods per millimeter, r_g. It remains to find the depth error along the camera ray.

Referring again to Figure 4.1, the ray through the projector lens is described by $y = x \tan(P)$ and the ray through the camera lens by $y = y_t ((x - x_c) / (x_t - x_c))$. Defining r as the range from the projector lens to the target, using

$$x_t = r \cos(P) \qquad y_t = r \sin(P)$$

and taking partial derivatives, the x and y errors in the target point solution, dx and dy, produced by an angle error dP, are found to be, under the reasonable assumption of small errors,

$$dx = (r^2 (\cos(P) - x_c / r) / x_c \sin(P)) dP$$
$$dy = (r^2 / x_c) dP$$

Define D to be the baseline distance between the projector and the camera, i.e. $D = x_c$. The standard deviation of the depth error is given in terms of the error in the angle P and geometrical parameters by

$$std(depth) = std(P) (r^2/D) (1+ ((\cos(P) - D / r) / \sin(P))^2)^{1/2}$$

Note the r^2/D range dependence of depth error for $r >> D$. This is characteristic of triangulation-based depth measurement systems. For this analysis, the target point is defined to be in the (x, y) plane and the grating is taken to be aligned so that it is invariant with z. Thus the target point is centered, and no z-error is caused by an error in angle P. More generally, the target point will not be centered and there will be an error in z. In normal practice, the z error (perpendicular to the paper in Figure 4.1) is small compared to the depth error calculated using these equations.

4.2 Quantization Effects on Phase Measurement Accuracy

In the Body Measurement System, images are acquired by CCD video cameras. Frame grabbers digitize the analog video signals. The effect of image amplitude quantization on the accuracy of phase measurement is analyzed in Section 4.2.1. Another source of quantization can be within the projected pattern itself. Projected pattern quantization occurs when the sinusoid is approximated by stepped intensity levels. This is addressed in Section 4.2.2, where it is shown that asymmetrical pattern quantization produces only half the phase measurement error as does symmetrical pattern quantization. In each case, we wish to know the effects of quantization so that we can specify the number of levels needed. The net phase measurement error variance is the sum of the contributing mutually uncorrelated phase measurement error variances.

4.2.1 Image Amplitude Quantization Effects

Eight-bit frame grabbers quantize the video signals into 256 levels of amplitude. At each image pixel that is to be processed for a depth solution, the sinusoidal pattern component is used to measure the phase of the projected pattern at that image

pixel, as shown in preceding sections. Because of varying surface reflectivity of the imaged subject, the number of quantization levels to which the sinusoidal component of the video signal is digitized will in general be less than the maximum number of levels available in the digitizer. In Ref. 3, the phase measurement error is analyzed in terms of the image signal-to-noise ratio (SNR). The accuracy of the depth solution is then analyzed in terms of the phase measurement error. Here we find the effect of image quantization on phase measurement accuracy. The result may be applied, in turn, to the depth solution analysis presented in Ref. 3 and summarized in the preceding.

If the digitizer is adjusted for zero-mean quantization error, then the error, or "noise", caused by quantization is distributed with uniform probability density $p(x)$, zero-mean over +/- one-half quantization increment. Thus $p(x)$ is unity over $-½ < x < ½$ and zero elsewhere. The variance of the image quantization noise, n_{iq}, is found from the statistical expectation,

$$\text{var}(n_{iq}) = E[x^2] = \int x^2 \, p(x) \, dx = 1/12$$

The image quantization noise n_{iq} standard deviation is therefore

$$\text{std}(n_{iq}) = 1 / (2 \sqrt{3}) \text{ quantization increment}$$

The peak-to-peak amplitude of the imaged sinusoidal pattern at a given pixel is $2b$. If this $2b$ sub-range of the image intensity is digitized to m levels, where m normally is substantially less than the number of levels to which the image is digitized, then each quantization increment corresponds to an amplitude increment of $2b / (m - 1)$. Expressed as an amplitude value, the standard deviation of the quantization noise becomes

$$\text{std}(n_{iq}) = b / ((m - 1) \sqrt{3})$$

As shown in Ref. 3, and summarized in preceding sections of this paper, the phase of the projected pattern is estimated from four image measurements, one at each of four different phase shifts of the projected pattern. The phase shift increments are nominally 90 degrees. Each of these image measurements contains amplitude quantization errors. Because there is no a priori deterministic relationship between the imaged sinusoid and the frame grabber digitization levels, the quantization errors among the four image measurements are taken to be uncorrelated.

An image quantization signal-to-noise power ratio (SNR_{iq}) can be defined for each image measurement. The variance of the sinusoidal pattern signal component is defined consistently with Ref. 3 as $b^2 / 2$. The signal to quantization noise variance, or power, ratio is therefore

$$SNR_{iq} = 3 (m - 1)^2 / 2$$

It is shown in Ref. 3 and summarized in the preceding sections that for uncorrelated noise components among the four image measurements the standard deviation of the error in measuring the phase p is

$$\text{std}(p) = 1 / (2 \sqrt{ SNR_{iq} }) \text{ radians, for } SNR_{iq} >> 1$$

The phase measurement error standard deviation is thus

$$\text{std}(p) = 1 / ((m - 1) \sqrt{6}) \text{ radians}$$

4.2.2 Pattern Sinusoid Quantization Effects

Similarly, if the projected pattern sinusoid is approximated by discrete steps into n levels, the standard deviation of the noise in each image that is caused by pattern quantization noise n_{pq} is

$$\text{std}(n_{pq}) = b / ((n - 1) \sqrt{3})$$

In the case of quantization of the pattern sinusoid, the digitization levels are deterministically related to the sinusoid by design, and in general the pattern quantization noises are not mutually uncorrelated. From Ref. 3, the phase measurement error variance is

$$\text{var}(p) = E[n_6^2 \cos^2(p) - 2\, n_5 n_6 \sin(p)\cos(p) + n_5^2 \sin^2(p)]$$

where

$$n_5 = (n_1 - n_3) / 2b \qquad n_6 = (n_4 - n_2) / 2b$$

and n_1 through n_4 are the noise values in the four image measurements. The images that are phase shifted by odd multiples of ninety degrees relative to one another are uncorrelated over a uniform phase distribution, because the phase increments corresponding to uniformly discretized amplitude increments will differ, thus randomizing the measurement errors between the images and producing zero correlation. Thus the middle term is zero, leaving

$$\text{var}(p) = E[n_6^2 \cos^2(p) + n_5^2 \sin^2(p)]$$

Further, it is clear that $E[n_6^2] = E[n_5^2]$ and so

$$\text{var}(p) = E[n_5^2]\,(\cos^2(p) + \sin^2(p)) = E[n_5^2]$$

The value of $E[n_5^2]$ will depend upon how the sinusoidal pattern is quantized.

First, consider symmetrical quantization, wherein the quantization levels are symmetrically disposed above and below the horizontal axis of the sinusoid such that the digitized sinusoid between 180 and 360 degrees is the negative of that between zero and 180 degrees. In this case,

$$n_1 = -n_3$$
$$n_5 = (n_1 - n_3) / 2b = n_1 / b$$
$$E[n_5^2] = \text{var}(n_1) / b^2$$

The standard deviation of n_1 was found above to be $b/((n-1)\sqrt{3})$, and so $\text{std}(p) = 1 / ((n-1)\sqrt{3})$, in radians, where the pattern quantization errors are set by design to zero mean. For comparison, note that this produces $\sqrt{2}$ times the phase measurement error standard deviation as does uncorrelated quantization noise, as was analyzed for image quantization in the preceding section.

Alternatively, consider an asymmetrical quantization, wherein the quantization levels are all shifted up by one-quarter of a quantization increment -- or the sinusoid may be shifted down by one quarter increment. Measurements between images shifted an odd multiple of 90 degrees are still uncorrelated. But in this case, when n_5 (or n_6) is formed as the difference between image points phase shifted by 180 degrees, the quantization error e, measured in quantization increments, is of the form

$$e = p / D, \text{ for } -D/2 < p < D/2$$

where p is the phase shift relative to a point of zero error at a given quantization level, and D is the width of that quantization level in radians. The quantization error thus ranges over +/- one-half quantization increment. For this alternative, the statistical expectation over a phase distribution uniform over –D/2 to D/2 is

$$E[e^2] = (1/D) \int e^2\, dp = 1/12 \text{ quantization increments squared}$$

Because the amplitude of each quantization increment is $2b/(n-1)$, and since n_5 is defined as the amplitude normalized by $2b$, $E[n_5^2] = 1 / (12(n-1)^2)$ and the standard deviation of the phase error is $\text{std}(p) = 1 / ((n-1)\sqrt{12})$ radians.

Note that the phase measurement error standard deviation under the asymmetrical pattern quantization alternative is only one-half of what it is under the symmetrical quantization alternative, and for comparison $1/\sqrt{2}$ times that of the uncorrelated noise case as analyzed for image amplitude quantization.

5. IMPLEMENTATION AND RESULTS

The output of the PMP process is a data cloud for each of the six sensor heads. See Figure 5.1. These individual data clouds are combined to create a composite point cloud of the whole body. Since each sensor head location and orientation has already been determined in a calibration process for the system, there is no zippering together of the individual sensor head point clouds.

By scanning a calibration object of known size and orientation, we are able to calculate the orientation of each sensor head with respect to the object. By placing the calibration object approximately where the subject will be standing, we also have a coarse correlation between the object and the subject to be scanned. This is important not only to assure correct coverage but to make sure the subject is within the depth of focus of each of the sensor heads. During system calibration, the calibration object is acquired using the acquisition sequence described in Section 3.2. Once the images have been acquired, they are processed and the resulting data points are determined with these data points being maintained in sensor head coordinates.

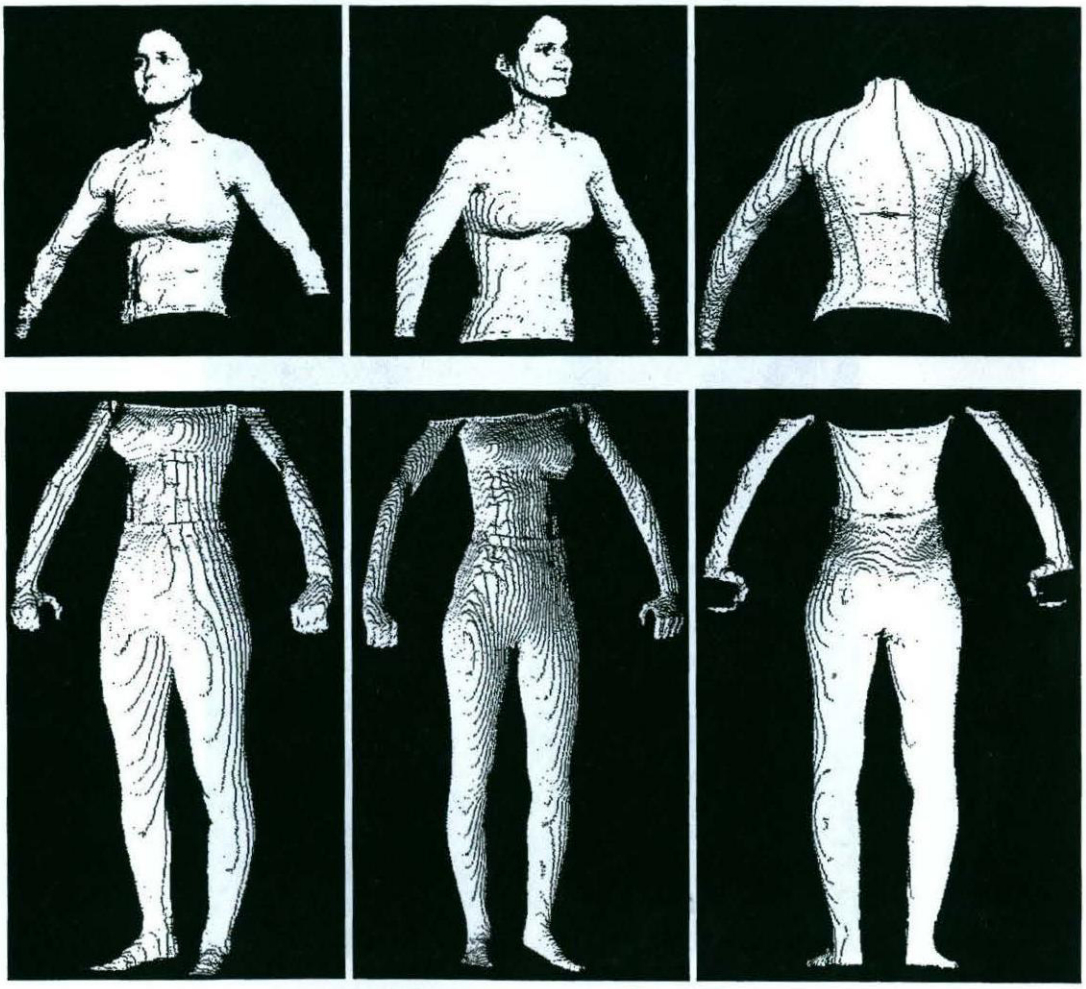

Figure 5.1 Six Individual Views of 3D Data Points

The system calibration process takes the area segment that is visible to each sensor and matches it to the calibration object using a minimization routine. Once the orientation of each sensor head has been determined, a transformation matrix is developed to transform the data into global coordinates. Figure 5.2 shows the resultant composite data set of a female model who was scanned with the BMS system. These data points are the raw calculated points without any smoothing or other post-processing.

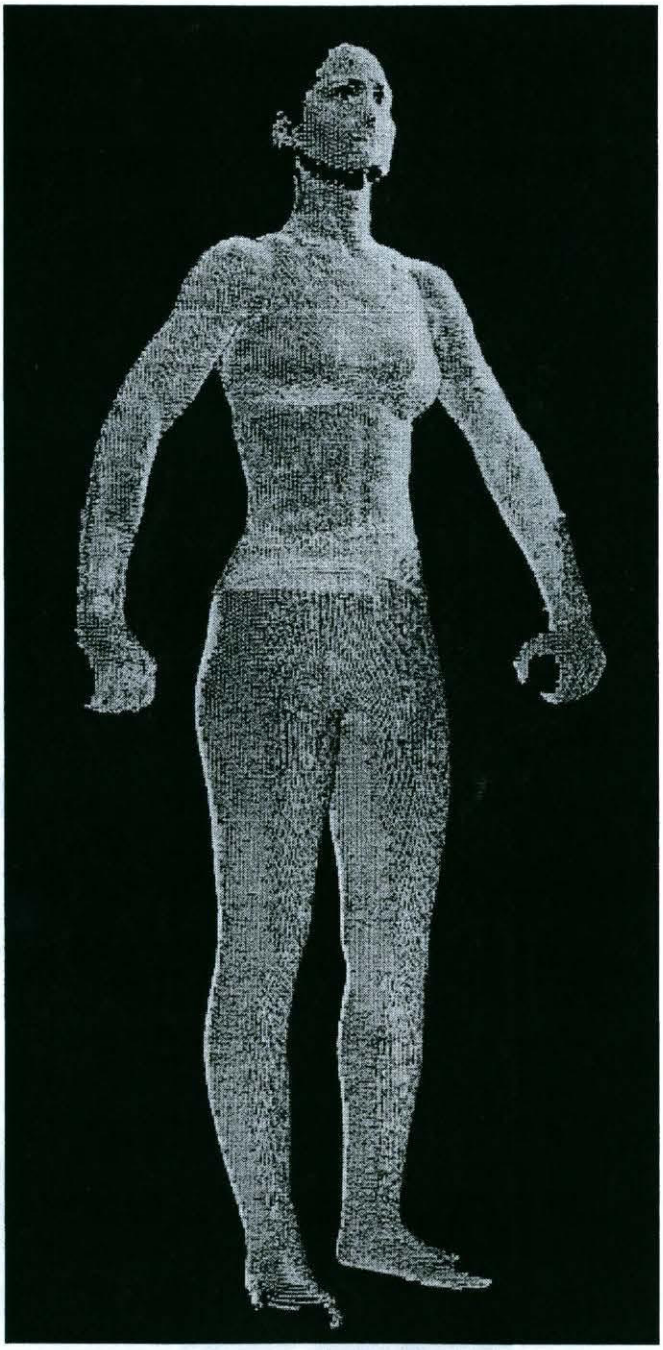

Figure 5.2 3D Composite Data Set

6. CONCLUSION

By close examination of the composite data set, it can be shown that good matching exists between the six views in the overlap regions. This is an indication that the system calibration is orienting the views properly and that the individual views are properly calibrated. Work is also progressing to extract measurements from the body data sets to alter garment patterns for making custom apparel.

ACKNOWLEDGEMENTS

This work was funded under a grant from the United States Department of Commerce.

REFERENCES

1. Halioua, M., L. Hsin-Chu, "Optical Three-Dimensional Sensing by Phase Measuring Profilometry", Optics and Lasers in Engineering, 0143-8166, pp.185-215, 1989.
2. Grindon, J. R., "Non-contact 3-D Surface Digitization of the Human Head", Proceedings of the National Computer Graphics Association Annual Conference, Atlanta, April, 1989.
3. Demers, M. H., and J. R. Grindon, J. D. Hurley, R. C. Wulpern, "Three Dimensional Surface Capture for Body Measurement using Projected Sinusoidal Patterns", Photonics West / Electronic Imaging 97, February, 1997 (SPIE Vol. 3023, pp. 13-25).